Mechanisms of reaction in cytochrome P450: hydroxylation of camphor in P450cam†

Jolanta Zurek,[a] Nicolas Foloppe,[b] Jeremy N. Harvey*[a] and Adrian J. Mulholland*[a]

Received 14th August 2006, Accepted 19th September 2006
First published as an Advance Article on the web 2nd October 2006
DOI: 10.1039/b611653a

The fundamental nature of reactivity in cytochrome P450 enzymes is currently controversial. Modelling of bacterial P450cam has suggested an important role for the haem propionates in the catalysis, though this finding has been questioned. Understanding the mechanisms of this enzyme family is important both in terms of basic biochemistry and potentially in the prediction of drug metabolism. We have modelled the hydroxylation of camphor by P450cam, using combined quantum mechanics/molecular mechanics (QM/MM) methods. A set of reaction pathways in the enzyme was determined. We were able to pinpoint the source of the discrepancies in the previous results. We show that when a correct ionization state is assigned to Asp297, no spin density appears on the haem propionates and the protein structure in this region remains preserved. These results indicate that the haem propionates are not involved in catalysis.

Introduction

Cytochrome P450 enzymes (P450s) are a large protein superfamily of haem monooxygenases. Humans possess 57 different active genes leading to expression of P450 enzymes,[1] and these enzymes are present in most living organisms in nature. These enzymes are involved in biosynthesis and in oxidation of xenobiotics. For example, P450s play a role in the synthesis of steroids, eicosanoids and other bioregulators.[2] The second function accounts for the strong interest in the biochemistry of human P450s among medicinal chemists and toxicologists,[3] as these enzymes metabolize the majority of administered drugs. Oxidation results in solubilization of compounds, facilitating their excretion from the body, and influencing their bioavailability. As this group of enzymes has a broad selectivity, it is important to understand their interactions with new medicinal compounds. Activation of prodrugs and conversion into toxins are among other pharmaceutically relevant effects of P450s.

The reactions catalysed by P450 enzymes have been extensively studied experimentally and computationally.[2,4–9] In most cases, the net transformation involves reduction of dioxygen, with incorporation of one oxygen atom into the substrate and reduction of the other to water:

$$NADPH + H^+ + O_2 + Sub \rightarrow NADP^+ + H_2O + Sub(O)$$

Detailed quantum mechanical (QM) studies have attempted to determine the nature and the reactivity of the active species in these enzymes, widely supposed to be a high-valent iron-oxo species, called Compound I (Cpd I—see Fig. 1). Calculations have been carried out on model systems and more recently on large models of cytochrome P450cam.

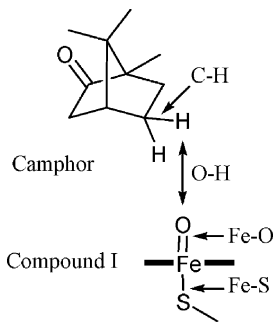

Fig. 1 Key species in the reaction of 5-*exo*-hydroxylation of camphor. Compound I is shown in a schematic way, with the haem ring shown as horizontal bars. The most important distances for the reaction are shown with arrows.

P450cam is a bacterial enzyme that catalyses 5-*exo*-hydroxylation of camphor. It was the first cytochrome P450 enzyme to be crystallized[10] and has been the subject of many subsequent experimental and computational studies. A large number of crystal structures are available for this enzyme, including one tentatively assigned to contain the active Cpd I species. The mechanism of the reaction in small models has been studied with electronic structure methods (as reviewed by Shaik *et al.*[7]) and more recently, the reaction in the protein has been investigated using hybrid quantum mechanical/molecular mechanical (QM/MM) approaches. Key species of the reaction are shown in Fig. 1, along with pointers for important atom distances. QM/MM methods allow the inclusion of the influence of the specific interactions in the protein on the reactants (*e.g.* including the effects of electronic polarization). They provide an excellent tool for investigating mechanisms of enzyme reactions. Initial QM/MM studies of P450cam focused on characterization of the active species,[11] whose spectroscopic properties were theoretically

[a]*Centre for Computational Chemistry, School of Chemistry, University of Bristol, Bristol, UK BS8 1TS. E-mail: Adrian.Mulholland@bristol.ac.uk, Jeremy.Harvey@bristol.ac.uk*
[b]*Vernalis (R & D) Ltd, Granta Park, Abington, Cambridge, UK CB1 6GB*
† Electronic supplementary information (ESI) available: Detailed reaction barriers, summary of key properties of the highest-energy points of each pathway. See DOI: 10.1039/b611653a

studied in more detail recently.[12] Studies of hydroxylation of camphor[13,14] followed, as well as analysis of the protein in its resting state[15] and of the enzyme–product complex,[16] as well as a study of the full catalytic cycle of the enzyme.[17] These calculations have raised a number of controversial issues concerning the nature of the active species and the reaction mechanism for this model enzymatic system.

Controversial proposals on P450 reactivity have arisen directly from QM/MM calculations on P450cam. Calculations found that a propionate sidechain on the haem group in the active species becomes partially oxidized, and carries unpaired electron density.[14,17] This was proposed to play an important role in the enzyme's catalytic properties. This was however not confirmed by other studies.[11,13] Also, different studies have produced rather different barrier heights and hence predicted reactivities for camphor oxidation. The two groups have published a joint paper recently[18] where they try to reconcile the conflicting results, but controversy still remains.[19,20]

Argument centres on the possible role of haem propionates in catalysis. A central question is whether there is unpaired electron density on these side chains of haem. The discrepancy between findings with apparently similar computational methods also questions whether studies which use a truncated model of haem can give a good description of a reaction surface, and potentially also the reliability of the QM/MM methods themselves.

We are interested in studying the metabolism of medicinal compounds with human P450 enzymes, including *e.g.* characterizing the Compound I active species in human drug-processing isoforms.[9] One important aim of this modelling is to predict the relative rate of oxidation of different substrates or of different sites in a given substrate, *e.g.* a drug molecule in a particular P450 isoform. Clearly, to develop predictive structure–reactivity relationships, an essential first stage is to establish the mechanisms of reactions in P450s. The hydroxylation of camphor in P450cam is an archetypal P450 reaction, making it particularly important to resolve the uncertainty in this case. It is also vital to resolve the apparent discrepancy between different calculations. The controversies are problematic in this respect since they suggest that differences in QM/MM procedures can lead to quite significantly different results. To have confidence in the results of mechanistic calculations, it is important to show that reproducible and consistent results can be obtained. Comparative studies of experimentally well characterized enzymes are particularly important for this.

A key question therefore is whether the differences between the calculated results are due to some difference between the (apparently similar) methods, or to some detail in the setup of the calculations. Only by reproducing different results can the causes of calculated differences be identified. Enzymes are notoriously complex, and great care must be applied in setting up any simulation of a protein. Uncertainties in experimental structures, or for example in the pK_as of ionizable groups, can make it difficult to choose a correct simulation setup unambiguously. It may be necessary to examine different possible systems to test the effects of such uncertainties. Tests of this sort could include examinations of the effects of structural differences, and alternative possible protonation states. Proteins are well known to have complex dynamics, giving rise to multiple different conformations, which may differ only subtly. The effects of structural variation can be explored, for example, by calculations on multiple structures derived from molecular dynamics simulations.[9,21] Different protein conformations can lead to different electronic structures in QM/MM computations,[9,11,22,23] and to somewhat different barrier heights to reaction.[21,24] Such variation is to be expected in proteins, and the steady state experimental rate will represent an average over many conformations. However, it is unlikely that thermal fluctuations should lead to qualitatively different chemical mechanisms for an enzyme. Nevertheless, these effects should be investigated. To examine this possibility and to probe to what extent QM/MM methodology can reproduce the known behaviour of this experimentally well-characterized system, we have investigated the reaction of hydroxylation of camphor using QM/MM procedures of the type we have previously applied to other metalloenzymes.[9,22] We investigate the electronic structure of the reactants and transition state, and compare results obtained in our calculations with previous findings, to identify sources of discrepancy. The importance of a protonation state of a nearby aspartate residue is shown, as it affects the structure of the protein, electronic state of the reactants and reactivity of the enzyme. These results provide additional insight into the accuracy of density-functional theory based QM/MM methods to describe reactivity in cytochrome P450 enzymes.

Computational methods

Protein preparation

The protein model was based on the crystal structure of P450cam from *Pseudomonas putida* in its complex with camphor[25] (PDB[26] entry 1DZ9, 1.9 Å resolution). The haem group in this crystal structure is represented by a putative active species—Cpd I. The system preparation was similar to approaches applied in the modelling of other enzymes.[9,22] Hydrogen atoms were added according to standard pK_a values, using the HBUILD[27] module of CHARMM[28] program version c27b2, and their position was then optimized. The CHARMM27[29] force field was used throughout. One residue not treated according to this rule was Asp297, where both protonation states were tested; the two different models are referred to in the text as the protonated and ionized models, respectively. If protonated, a hydrogen atom was added to the OD2 oxygen, forming a hydrogen bond between OD2 and the O2A atom of the haem propionate. As shown in Fig. 2, any other possible placement of the proton would not lead to a favourable geometry for the hydrogen bond. Histidine tautomers were assigned on the basis of the local hydrogen bonding environment. The protein was then truncated to a 25 Å sphere centred around the haem iron. In pure forcefield (not QM/MM) calculations, all polar residues (Asp, Lys, Glu, Arg) located 20 Å or more from the centre of the system (buffer region) were neutralized, unless they were forming salt bridges with charged residues in the inner region. This led to a system with an overall charge of −1e for the ionized model, and with no charge for the protonated model. A non-bonded cutoff of 13 Å was used in the MM calculations for preparation of the system before QM/MM calculations.

The system was then immersed in a 25 Å sphere of water (CHARMM TIP3P[30] model), centred on the haem iron atom. All overlapping water molecules, *i.e.* whose oxygen atom was 2.6 Å or closer to existing heavy atoms, were deleted. The water was then

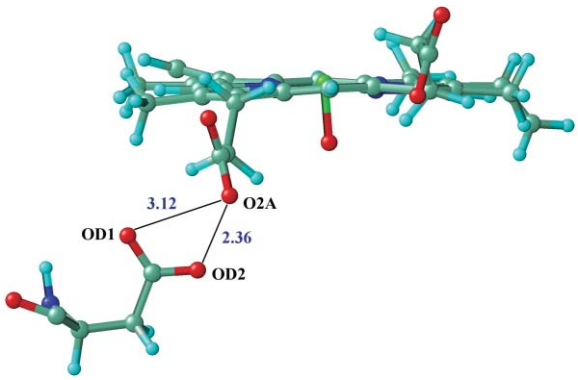

Fig. 2 Arrangement of oxygen atoms in Asp297 and A-propionate of haem group. If added, hydrogen atom was placed between atoms O2A and OD2. The positions of atoms O2A and OD2 clearly indicate a very favourable hydrogen bond between them; any other oxygen atom combinations would give a less optimal geometry of the hydrogen bond. The distances between atoms are given in Å, atom names are as in the PDB file.

optimized and equilibrated (with other atoms fixed) in a stochastic boundary molecular dynamics (SBMD)[31] simulation using full Newtonian dynamics for water molecules within a distance of 20 Å from the haem iron, and Langevin dynamics for the remaining water molecules. A deformable boundary potential was used to keep water oxygen atoms within 25 Å of the iron. The whole system was then minimized and equilibrated for 100 ps with SBMD. The haem group (represented with Compound I force field parameters) was frozen in all MM calculations, with other atoms within the 20 Å sphere free to move, and protein atoms beyond 20 Å harmonically restrained to their initial positions (with force constants increasing with the distance from the centre of the system[32,33]). The energy of the system was then minimized. This optimized geometry was used as a starting point for three independent 100 ps SBMD runs (following the same protocol as described above). The final geometry from each run was minimized by MM, leading to three independent starting geometries for both the ionized and the protonated models. Full details of protein preparation, including definition of non-standard forcefield residues, are given in the ESI.†

QM/MM calculations

QM/MM calculations used density functional theory (DFT) with the B3LYP functional to describe the QM region and the CHARMM 27 forcefield[29] for the MM region. The molecular mechanical part of the calculations was carried out using Tinker,[34] with atoms outside a 20 Å sphere centred on the iron atom held fixed. The DFT part of the calculations was carried out using Jaguar 4,[35] and included the field generated by the point charges on the MM atoms. In most calculations, the standard Los Alamos effective core potential and associated double-ζ contracted basis set LACVP was used on the iron atom, and the 6-31G basis set on all other atoms (BS I). Additional calculations were carried out using the larger BS II, which includes a triple-ζ contraction of the LACVP basis set (LACV3P**) on iron and the 6-31G** basis on other atoms. These methods have been shown to treat such systems well.[8,13,36,37] Two QM regions were investigated. The first (QM1) included the camphor molecule, the methyl thiolate part of the haem-coordinating cysteine and the unsubstituted porphyrin ring. In QM2, all substituents on the haem ring were included. All C–C bonds at the boundary of the QM and MM regions were capped with hydrogen 'link atoms'. MM charges on the atom replaced by the link atom and some atoms directly connected to it were set to zero, to avoid unphysical effects.[9] QM regions 1 and 2 consisted of 70 and 106 atoms, respectively. BS I and QM1 were used unless mentioned otherwise. Coupling between the QM and MM regions, and energy minimization of the QM system, was carried out with the QoMMMa program.[36] No cutoffs for electrostatic or van der Waals nonbonded interactions were used in QM/MM calculations. Reaction profiles were generated by carrying out a series of QM/MM minimizations with the distance between the Cpd I oxygen and the reacting camphor hydrogen restrained to different values. This reaction coordinate has been applied successfully in previous studies.[13]

Results and discussion

The key step in the reaction mechanism, and the one for which the different computations have shown the largest discrepancies, is the hydrogen abstraction by Cpd I. We therefore focus on this step only. In the first part of our work, three independent reaction pathways were calculated for the protein with Asp297 in its ionized state. The starting geometries were derived from molecular dynamics simulations. The position of camphor remains stable during the dynamics and does not change much (average RMS value of heavy atoms of camphor with respect to starting MD conformation were 0.5, 0.43 and 0.44 Å for the respective pathways). We observe a water molecule hydrogen-bonding to the Cpd I oxygen atom throughout the duration of each MD simulation and in all QM/MM optimizations. The average reaction barrier was 15.3 ± 0.35 kcal mol^{-1}. The key reaction distances in the average geometry of the transition state (TS) were Fe–S: 2.56 Å, Fe–O: 1.78 Å, O–H: 1.24 Å, C–H: 1.38 Å. The TS geometry is very similar to that found by others,[13] although here the TS is located earlier with respect to hydrogen transfer (the O–H distance is 1.24 Å, compared to 1.15 Å). A water molecule stays hydrogen-bonded to Cpd I oxygen throughout the reaction. One of these pathways was then reoptimized using the larger QM2 which includes the haem side chains in the QM region. Exact energy barriers and geometrical details of transition states are given in the ESI.†

At the initial geometry of the QM/MM optimization of the reactant complex (the optimized structure from QM/MM using QM1), a small amount of unpaired electron density was observed on the haem propionates (0.008 e and 0.036 e on the oxygen atoms) when calculated with QM2. After QM/MM reoptimization using QM2, the small changes in geometry due to the different location of the QM–MM boundary lead to some loss of spin density on the propionate (0.003 e and 0.033 e). This small level of spin density is also observed to diminish at all subsequent geometries along the reaction pathway (spin densities of 0.0003 e and 0.0029 e at the transition state, and 0.0008 e and 0.01 e in the product complex). The barrier along the QM2 reaction pathway is 2.2 kcal mol^{-1} higher than that obtained with QM1,

but the optimized geometries along this pathway are not changed significantly.

The observation of only very small spin densities on the haem propionate groups after optimization is consistent with results obtained by Thiel *et al.*[13] However, in other QM/MM studies by Guallar *et al.*,[14] extensive spin density is obtained on these groups. There is a significant difference between our system setup and that used in the latter study. Our starting geometries for QM/MM pathway minimization are derived from molecular dynamics equilibration of all atoms within a large sphere centred around the haem group, whereas Guallar *et al.*[14,17] used the crystal structure directly without preliminary equilibration. To assess the impact of this different system preparation, a calculation on the Compound I–camphor complex was carried out using a starting structure derived from the crystal structure by truncation, solvation and water equilibration, while keeping all coordinates of the protein fixed. A QM/MM single point calculation using the large QM2 region led to a wavefunction with significant spin density on the A-propionate (0.53 e on one of the oxygens and 0.05 e on the other). After QM/MM minimization, slightly reduced spin densities of 0.28 e and 0.03 e, respectively, were found.

The key structural difference between the crystal structure and the equilibrated structure appears to be the movement of a potentially negatively charged group, Asp297. In the crystal structure the carboxylate group of this residue is located (perhaps surprisingly) close to the negatively charged propionate. This interaction, which might be unexpected, is a common characteristic of crystal structures of this enzyme. The distance between the two closest interacting oxygen atoms in the crystal structure is 2.36 Å. Such an unusually short distance appears in several high-resolution crystal structures of P450cam, but in the majority of structures it is in the range of 2.5–2.8 Å (see Table 1 for examples, and Table S1 in the ESI† for a more extensive list). The short separations observed experimentally are indicative of a hydrogen bond between Asp297 and the propionate. Poisson–Boltzmann continuum electrostatic calculations[38] suggested that one of the carboxylates is protonated. Where neither group is protonated, as in our first set of calculations (and in some previous work[13,14]), Coulombic repulsion by Asp297 effectively decreases the electron affinity of the A-propionate carboxylate group, facilitating partial electron transfer to the haem ring. This is especially strong in the unequilibrated crystal structure, because of the short distance between the two groups. Clearly, the presence of a negative charge on Asp297 could potentially have a significant impact on the electronic structure of Compound I.

Table 1 Examples of O–O distances between the A-propionate oxygen of the haem group and a carboxylate oxygen of Asp297. The shortest of four possible distances is given. For measurements in all P450cam structures present in the PDB database with a resolution of 2.00 Å or better, refer to Table S1 in the ESI

PDB code	Subunit A/Å	Subunit B[a]/Å
1AKD	2.77	
1DZ6	2.34	2.69
1DZ9	2.36	2.73
1GEK	2.59	
1GEM	2.55	
1IWI	2.57	
1IWK	2.69	
1K2O	2.64	2.69
1O76	2.39	2.67
1PHA	2.63	
1PHD	2.78	
1QMQ	2.66	3.55[b]
1RE9	2.69	
1T85	2.49	
2A1O	2.58	2.41
2CPP	2.74	

[a] In the cases where two protein units were present in the coordinate file, distances for each unit are given. [b] The number corresponds to an alternative conformation of Asp297 side chain in subunit A, not to Asp297 in subunit B.

Our QM/MM calculations and molecular dynamics (MD) simulations provide a strong indication that Asp297 is protonated, and must be treated as such to achieve consistency with the experimental structures. MD simulations treating both Asp297 and the A-propionate as negatively charged show a clear and significant increase in distance between the two groups (as described below). The impact of MD equilibration is very different for the models treating Asp297 as protonated or ionized. For each ionization state, three independent MD simulations were carried out. In the case of the ionized model, the shortest O–O contact (initially 2.36 Å) significantly increased in length during the early stages of the MD run, then oscillated around 3.6–4.0 Å. In the resulting conformation, the carboxylate group of Asp297 points away from the haem propionate, thereby minimizing the repulsive interaction between these two carboxylate groups (as shown in Fig. 3).

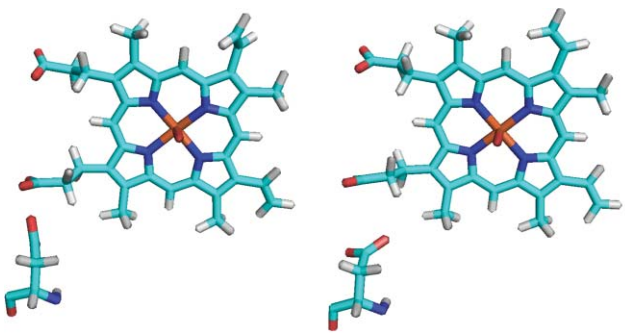

Fig. 3 Difference in the conformation of ionized Asp297 between the initial conformation (on the left) and in the equilibrated system (on the right).

This distance does not decrease when these structures are used in QM/MM calculations with QM region 1, and changes by no more than 0.05 Å with QM region 2. Similarly, when the unequilibrated protein (crystal) structure was subjected to QM/MM minimization (using larger QM region 2) in which both carboxylates were treated as charged, the distance between their oxygen atoms also increased: from 2.36 Å to 3.9 Å. Clearly, when Asp297 is ionized, the experimentally observed interaction with the A-propionate is not preserved. Further demonstration of the sensitivity to the O–O distance of the system with both Asp297 and the propionate charged was provided by further tests with the large QM region. These reinforced the conclusion that a short O–O distance can lead to significant spin density on the propionate when both partners are charged. One QM/MM optimization (pathway 2) of this system produced a conformation in which the Asp297-propionate O–O distance was 3.05 A. This

showed spin density on the haem propionate oxygens of 0.13 e and 0.11 e. Roughly the same amount of spin density remains on the propionate throughout this pathway, with the values in the product complex being 0.1 e and 0.08 e. In all the simulations where Asp297 was protonated, its conformation remained very stable. It formed a hydrogen bond with the propionate, with an O–O distance close to 2.7 Å. This distance is in agreement with a number of crystal structures of P450cam, although slightly longer than the value in the crystal structure we used as a starting point (2.36 Å). The exact O–O separation is not known exactly, due to variability in crystal structures, but available data clearly indicates the presence of a hydrogen bond. In short, only molecular dynamics simulations in which Asp297 is protonated lead to a stable conformation resembling the crystal structure. It should be noted that the CHARMM 27[29] force field was optimized to accurately represent protein structure and interaction.

A second crucial question is whether these differences in the electrostatic environment of the haem group (ionized *versus* protonated forms of Asp297) have important effects on reactivity. Three reaction pathways for hydrogen abstraction were calculated for the models with protonated Asp297 (using QM region 1) and compared with results for the ionized model, described above. Table 2 shows the average reaction barrier height for both models, and average key distances (as shown in Fig. 1).

The reaction barrier is elevated by about 3 kcal mol^{-1} for the protonated model; the spin density on sulfur is a little higher than in the case of (the optimized) ionized model, and accordingly the Fe–S bond in slightly lengthened. The structure of the transition state does not change much in the protonated model, with average key atomic distances different by less than 0.03 Å. One of the pathways was also recalculated with QM region 2. This led to an increase in barrier height by *ca.* 2.5 kcal mol^{-1} with little change in structure. No spin density was found on the haem propionates at any point along the reaction coordinate in any of these calculations.

The 3 kcal mol^{-1} energy difference for the reaction in models with ionized and protonated aspartate can probably be attributed to a slightly different arrangement of the protein environment after protein equilibration. The geometry and electronic structure of the QM region at the highest points along the energy profiles are very similar in all cases, so the different protonation state does not seem to lead to a major chemical change explaining the slightly higher barrier. It is possible that the difference is merely due to the fact that we are comparing results calculated as an average over three conformations only, and reflects the intrinsic variability from one protein conformation to another.[21,39] Longer equilibration and calculation of more QM/MM energy profiles in the two cases might lead to average barriers more similar to each other. It is also possible that if Compound I could be generated in the presence of an ionized Asp297, then it would be slightly more reactive than in the protonated form. However, as noted above, the structural evidence suggests that the ionized form is not accessible. It should also be noted that the close contact of an acidic residue with a haem propionate chain seems to be a unique feature of P450cam. No such contact is present in any of the crystallized structures of human P450 enzymes.[40–46] This means that there is no corresponding problem in assigning the ionization state when modelling human P450s[9] and their reactions with drugs. It also suggests that the presence of an ionized acidic residue close to the haem group cannot play an important catalytic role.

Table 2 Average values for the energy barrier of hydrogen abstraction from camphor, key distances and spin density on sulfur of the highest-energy geometry on the pathway

Property	Ionized model	Protonated model
Reaction barrier/kcal mol^{-1}	15.3	18.3
O–H distance/Å	1.24	1.22
C–H distance/Å	1.37	1.4
Fe–O distance/Å	1.78	1.79
Fe–S distance/Å	2.56	2.58
Spin density on sulfur/e	0.21	0.27

The average QM/MM barriers are 15.3/18.3 kcal mol^{-1} for the ionized/protonated models, respectively. The use of a larger QM region and/or a larger basis set slightly increase these values, so that our best estimate of the activation barrier for reaction in the protonated form is *ca.* 20 kcal mol^{-1}. How consistent is this with other results? First of all, our results are very consistent with the previous computational work of Shaik *et al.*,[11,13] despite using a completely independent system set-up and a different QM/MM procedure. This is important as it shows that despite the complexity of these metalloenzyme systems, careful QM/MM work leads to reproducible results.

On the experimental side, there is only indirect evidence concerning the barrier height. Kinetic studies suggest that hydrogen atom abstraction is not rate-limiting so the measured[47] k_{cat} value of 66 s^{-1} is only a lower limit of the rate constant for the step we are studying. Cryogenic studies of a Compound I precursor in P450cam led to the product complex on a timescale of several seconds, without it being possible to detect an intermediate Compound I. This suggests that the latter is a very short lived species, with a rate constant for hydrogen abstraction from substrate at 200 K of close to 1 s^{-1} or higher. At room temperature, attempts to generate Compound I in a number of P450 isoforms suggest that it decays by electron transfer from various oxidizable protein side-chains on a timescale of a few milliseconds.[48–50] These experiments are carried out in the absence of substrate and hence with water in the active site pocket, which may enhance this electron transfer process. Nevertheless, for hydrogen abstraction to dominate over electron transfer in the presence of substrate, the rate constant should probably be at least of the order of 1000 s^{-1}. In contrast to these observations, decay of Compound I in bacterial CYP119[51] is not significantly faster in the presence of substrate than in its absence.

Nevertheless, all these results suggest a relatively low barrier to hydrogen atom abstraction. Direct application of the Eyring equation using the *ca.* 1 s^{-1} rate constant at 200 K gives a free energy of activation of *ca.* 11 kcal mol^{-1}, while the value of 1000 s^{-1} at room temperature corresponds to a value of *ca.* 13 kcal mol^{-1}. The k_{cat} value of 66 s^{-1} suggests the free energy barrier must be lower than 15 kcal mol^{-1}. All these values are much lower than our calculated barrier. However, the latter is an energy barrier, not a free energy, so that some corrections are needed in order to compare with experiment.

First, the zero-point energy (ZPE) at the TS is considerably reduced compared to the reactant complex. Shaik *et al.*[13] estimated the ZPE correction to be ~4 kcal mol^{-1}. Hydrogen atom tunnelling[52] would lower the apparent free energy of activation.

In favourable cases, with extensive tunnelling, this effect can lower the activation free energy by up to 4.5 kcal mol^{-1}. At first sight, such a large effect is not expected for P450cam, as experimental isotope effects have been known for some time to be fairly small. However, these apparent isotope effects are misleading because as already stated, H atom abstraction is not rate-limiting. Newer experimental work shows that the underlying k_H/k_D isotope effect for the abstraction step can be as large as 15.[53,54] This should correspond to significant tunnelling, as expected for a process involving H atom transfer, and should thereby lead to a decreased activation free energy. The extent of this lowering is not clear but it is reasonable to assume it could be of the order of 2 kcal mol^{-1}. Finally, entropic effects contribute to the experimental activation free energy. The loss of some rotational and translational entropy of the camphor substrate will be counterbalanced to some extent by the looser vibrations of the transferring H atom, and the net effect is likely to be small.

The net result of these corrections is a predicted activation free energy of the order of 14 kcal mol^{-1}. Considering the possible error associated with the B3LYP DFT method, the calculated barrier is consistent with experiment, if at the higher end of the possible range. This conclusion was also reached in previous QM/MM studies.[13]

Conclusions

In this paper, we have studied the hydrogen abstraction step in the hydroxylation of camphor by P450cam. As well as calculating reaction pathways using QM/MM methods, we have used molecular dynamics methods to examine the structure of the Compound I enzyme–substrate complex, and determined the electronic structure of this species. Previous QM/MM work by other groups[13,14] led to inconsistent predictions concerning the presence of spin density on the haem A-propionate sidechain. We have found that this spin density is only found when a charged aspartate is in the proximity of the propionate. This is most significant when the unrelaxed crystal structure of the protein is used—geometry optimization and molecular dynamics equilibration lead to structures with reduced spin density.

Our results also show that a much better model is obtained when using a protonated Asp297 residue, as this preserves the protein conformation around the haem propionates during MD equilibration and QM/MM optimization. In this case we do not observe any spin density on the haem propionates. This agrees with results obtained before by others.[13,18] In such a system, the reaction proceeds with an average energy barrier of 18.3 kcal mol^{-1}. Inclusion of the full haem unit into the quantum calculations slightly increases the barrier, but does not significantly change the geometry of the transition state. Our calculated barrier heights are consistent with rapid hydrogen atom abstraction by Compound I provided that a correction for zero-point energy is included and that some allowance is made for hydrogen atom tunnelling.

Acknowledgements

JZ would like to thank Dr Christine M. Bathelt for helpful discussions and Vernalis plc for funding. AJM thanks the IBM High Performance Computing Life Sciences Outreach Programme, BBSRC and EPSRC for support. JNH is an EPSRC Advanced Research Fellow.

References

1 D. R. Nelson, D. C. Zeldin, S. M. G. Hoffman, L. J. Maltais, H. M. Wain and D. W. Nebert, *Pharmacogenetics*, 2004, **14**, 1–18.
2 F. P. Guengerich, *Chem. Res. Toxicol.*, 2001, **14**, 611–650.
3 A. J. Mulholland, *Drug Discovery Today*, 2005, **10**, 1393–1402.
4 I. G. Denisov, T. M. Makris, S. G. Sligar and I. Schlichting, *Chem. Rev.*, 2005, **105**, 2253–2277.
5 M. J. Coon, *Annu. Rev. Pharmacol. Toxicol.*, 2005, **45**, 1–25.
6 F. P. Guengerich, *Drug Metab. Rev.*, 2004, **36**, 159–197.
7 S. Shaik, D. Kumar, S. P. de Visser, A. Altun and W. Thiel, *Chem. Rev.*, 2005, **105**, 2279–2328.
8 C. M. Bathelt, L. Ridder, A. J. Mulholland and J. N. Harvey, *Org. Biomol. Chem.*, 2004, **2**, 2998–3005.
9 C. M. Bathelt, J. Zurek, A. J. Mulholland and J. N. Harvey, *J. Am. Chem. Soc.*, 2005, **127**, 12900–12908.
10 T. L. Poulos, B. C. Finzel and A. J. Howard, *J. Mol. Biol.*, 1987, **195**, 687–700.
11 J. C. Schoneboom, H. Lin, N. Reuter, W. Thiel, S. Cohen, F. Ogliaro and S. Shaik, *J. Am. Chem. Soc.*, 2002, **124**, 8142–8151.
12 J. C. Schoneboom, F. Neese and W. Thiel, *J. Am. Chem. Soc.*, 2005, **127**, 5840–5853.
13 J. C. Schoneboom, S. Cohen, H. Lin, S. Shaik and W. Thiel, *J. Am. Chem. Soc.*, 2004, **126**, 4017–4034.
14 V. Guallar, M. H. Baik, S. J. Lippard and R. A. Friesner, *Proc. Natl. Acad. Sci. USA*, 2003, **100**, 6998–7002.
15 J. C. Schoneboom and W. Thiel, *J. Phys. Chem. B*, 2004, **108**, 7468–7478.
16 H. Lin, J. C. Schoneboom, S. Cohen, S. Shaik and W. Thiel, *J. Phys. Chem. B*, 2004, **108**, 10083–10088.
17 V. Guallar and R. A. Friesner, *J. Am. Chem. Soc.*, 2004, **126**, 8501–8508.
18 A. Altun, V. Guallar, R. A. Friesner, S. Shaik and W. Thiel, *J. Am. Chem. Soc.*, 2006, **128**, 3924–3925.
19 V. Guallar and B. Olsen, *J. Inorg. Biochem.*, 2006, **100**, 755–760.
20 A. Altun, S. Shaik and W. Thiel, *J. Comput. Chem.*, 2006, **27**, 1324–1337.
21 F. Claeyssens, K. E. Ranaghan, F. R. Manby, J. N. Harvey and A. J. Mulholland, *Chem. Commun.*, 2005, 5068–5070.
22 C. M. Bathelt, A. J. Mulholland and J. N. Harvey, *Dalton Trans.*, 2005, 3470–3476.
23 J. N. Harvey, C. M. Bathelt and A. J. Mulholland, *J. Comput. Chem.*, 2006, **27**, 1352–1362.
24 Y. K. Zhang, J. Kua and J. A. McCammon, *J. Phys. Chem. B*, 2003, **107**, 4459–4463.
25 I. Schlichting, J. Berendzen, K. Chu, A. M. Stock, S. A. Maves, D. E. Benson, B. M. Sweet, D. Ringe, G. A. Petsko and S. G. Sligar, *Science*, 2000, **287**, 1615–1622.
26 http://www.pdb.org.
27 A. T. Brunger and M. Karplus, *Proteins: Struct., Funct., Genet.*, 1988, **4**, 148–156.
28 B. R. Brooks, R. E. Bruccoleri, B. D. Olafson, D. J. States, S. Swaminathan and M. Karplus, *J. Comput. Chem.*, 1983, **4**, 187–217.
29 A. D. MacKerell, D. Bashford, M. Bellott, R. L. Dunbrack, J. D. Evanseck, M. J. Field, S. Fischer, J. Gao, H. Guo, S. Ha, D. Joseph-McCarthy, L. Kuchnir, K. Kuczera, F. T. K. Lau, C. Mattos, S. Michnick, T. Ngo, D. T. Nguyen, B. Prodhom, W. E. Reiher, B. Roux, M. Schlenkrich, J. C. Smith, R. Stote, J. Straub, M. Watanabe, J. Wiorkiewicz-Kuczera, D. Yin and M. Karplus, *J. Phys. Chem. B*, 1998, **102**, 3586–3616.
30 W. L. Jorgensen, J. Chandrasekhar, J. D. Madura, R. W. Impey and M. L. Klein, *J. Chem. Phys.*, 1983, **79**, 926–935.
31 C. L. Brooks and M. Karplus, *J. Chem. Phys.*, 1983, **79**, 6312–6325.
32 A. J. Mulholland and W. G. Richards, *Proteins*, 1997, **27**, 9–25.
33 J. Zurek, A. L. Bowman, W. A. Sokalski and A. J. Mulholland, *Struct. Chem.*, 2004, **15**, 405–414.
34 J. W. Ponder, *TINKER-Software Tools for Molecular Design*, Washington University, St. Louis, MO, 2003.
35 Jaguar *Jaguar*, Schrodinger, Inc., Portland, OR, 2000.
36 J. N. Harvey, *Faraday Discuss.*, 2004, **127**, 165–177.
37 N. Strickland, A. J. Mulholland and J. N. Harvey, *Biophys. J.*, 2006, **90**, L27–L29.

38 V. Lounnas and R. C. Wade, *Biochemistry*, 1997, **36**, 5402–5417. Due to a typographical error, Asp297 was denoted as Asp197 in the text.
39 Y. K. Zhang, J. Kua and J. A. McCammon, *J. Am. Chem. Soc.*, 2002, **124**, 10572–10577.
40 P. A. Williams, J. Cosme, A. Ward, H. C. Angova, D. M. Vinkovic and H. Jhoti, *Nature*, 2003, **424**, 464–468.
41 P. Rowland, F. E. Blaney, M. G. Smyth, J. J. Jones, V. R. Leydon, A. K. Oxbrow, C. J. Lewis, M. G. Tennant, S. Modi, D. S. Eggleston, R. J. Chenery and A. M. Bridges, *J. Biol. Chem.*, 2006, **281**, 7614–7622.
42 J. K. Yano, M. H. Hsu, K. J. Griffin, C. D. Stout and E. F. Johnson, *Nat. Struct. Molec. Biol.*, 2005, **12**, 822–823.
43 J. K. Yano, M. R. Wester, G. A. Schoch, K. J. Griffin, C. D. Stout and E. F. Johnson, *J. Biol. Chem.*, 2004, **279**, 38091–38094.
44 M. R. Wester, J. K. Yano, G. A. Schoch, C. Yang, K. J. Griffin, C. D. Stout and E. F. Johnson, *J. Biol. Chem.*, 2004, **279**, 35630–35637.
45 P. A. Williams, J. Cosme, D. M. Vinkovic, A. Ward, H. C. Angove, P. J. Day, C. Vonrhein, I. J. Tickle and H. Jhoti, *Science*, 2004, **305**, 683–686.
46 G. A. Schoch, J. K. Yano, M. R. Wester, K. J. Griffin, C. D. Stout and E. F. Johnson, *J. Biol. Chem.*, 2004, **279**, 9497–9503.
47 M. M. Purdy, L. S. Koo, P. R. O. de Montellano and J. P. Klinman, *Biochemistry*, 2004, **43**, 271–281.
48 V. Schunemann, C. Jung, A. X. Trautwein, D. Mandon and R. Weiss, *FEBS Lett.*, 2000, **479**, 149–154.
49 C. Jung, V. Schunemann and F. Lendzian, *Biochem. Biophys. Res. Commun.*, 2005, **338**, 355–364.
50 C. Jung, V. Schunemann, F. Lendzian, A. X. Trautwein, J. Contzen, M. Galander, L. H. Bottger, M. Richter and A. L. Barra, *Biol. Chem.*, 2005, **386**, 1043–1053.
51 M. Newcomb, R. Zhang, R. E. P. Chandrasena, J. A. Halgrimson, J. H. Horner, T. M. Makris and S. G. Sligar, *J. Am. Chem. Soc.*, 2006, **128**, 4580–4581.
52 L. Masgrau, A. Roujeinikova, L. O. Johannissen, P. Hothi, J. Basran, K. E. Ranaghan, A. J. Mulholland, M. J. Sutcliffe, N. S. Scrutton and D. Leys, *Science*, 2006, **312**, 237–241.
53 J. A. Krauser and F. P. Guengerich, *J. Biol. Chem.*, 2005, **280**, 19496–19506.
54 L. Higgins, G. A. Bennett, M. Shimoji and J. P. Jones, *Biochemistry*, 1998, **37**, 7039–7046.